Supplementary Information

SAR-based approach to explore in silico ferrocene analogues as the potential inhibitors of major viral proteins of SARS-CoV-2 virus and human Ca^{2+}-channel blocker

Maynak Pal[a], Dulal Musib[a] & Mithun Roy[a,]*

Department of Chemistry, National Institute of Technology Manipur, Langol 795 004, Manipur, India

*E-mail: mithunroy@nitmanipur.ac.in

Received 09 November 2021; revised and accepted 28 March 2022

Table S1: Grid Dimensions used in molecular docking of major viral proteins of SARS-CoV-2.							
Protein	**Grid dimensions**				**Grid center**		
	X	**Y**	**Z**	**Spacing**	**X**	**Y**	**Z**
Spike protein	126	126	100	0.375	287.854	252.491	345.512
RdRp protein	126	80	100	0.375	103.434	97.322	112.476
M_{pro} protein	126	126	126	0.375	11.554	-0.133	5.627
N protein	126	126	126	0.675	12.76	-12.033	-24.877
Ca channel protein	80	84	126	0.375	176.642	168.446	188.42

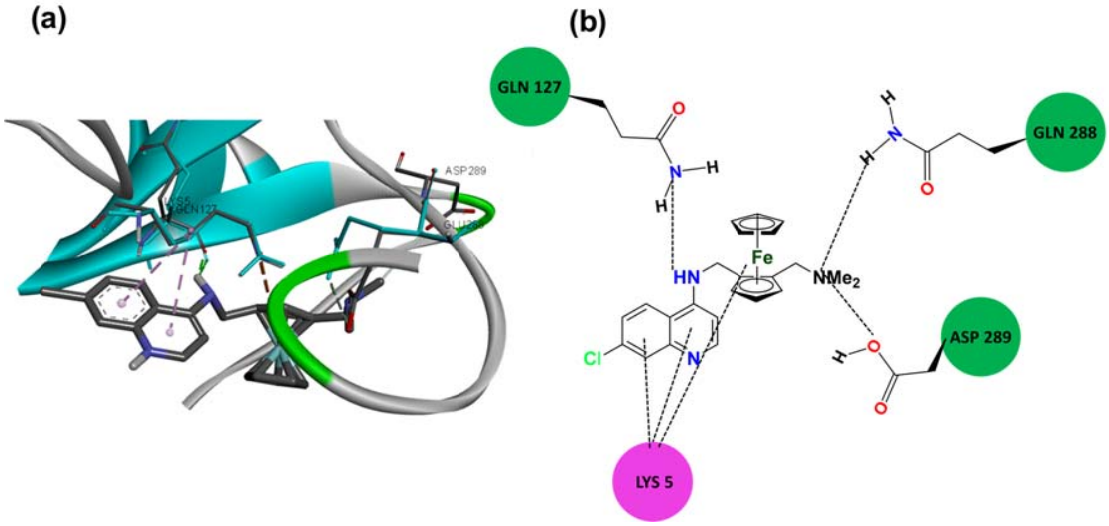

Fig. S1 - The best dock pose exhibiting non-covalent interactions between ferroquine and the M_{pro} protein of SARS-CoV-2. (b) Schematic representation of showing the all the non-covalent interactions with GLN127, LYS5, ASP289, GLN288 residues.

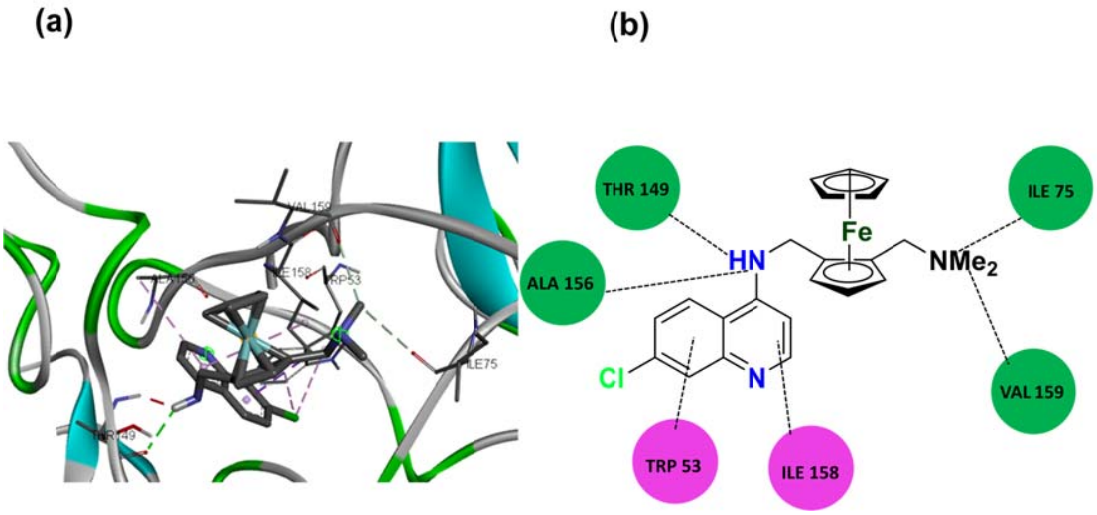

Fig. S2 - The best dock pose exhibiting non-covalent interactions between ferroquine and the N protein of SARS-CoV-2. (b) Schematic representation of showing the all the non-covalent interactions with ALA156, THR149, ILE75, VAL159, TRP53, ILE158 residues.

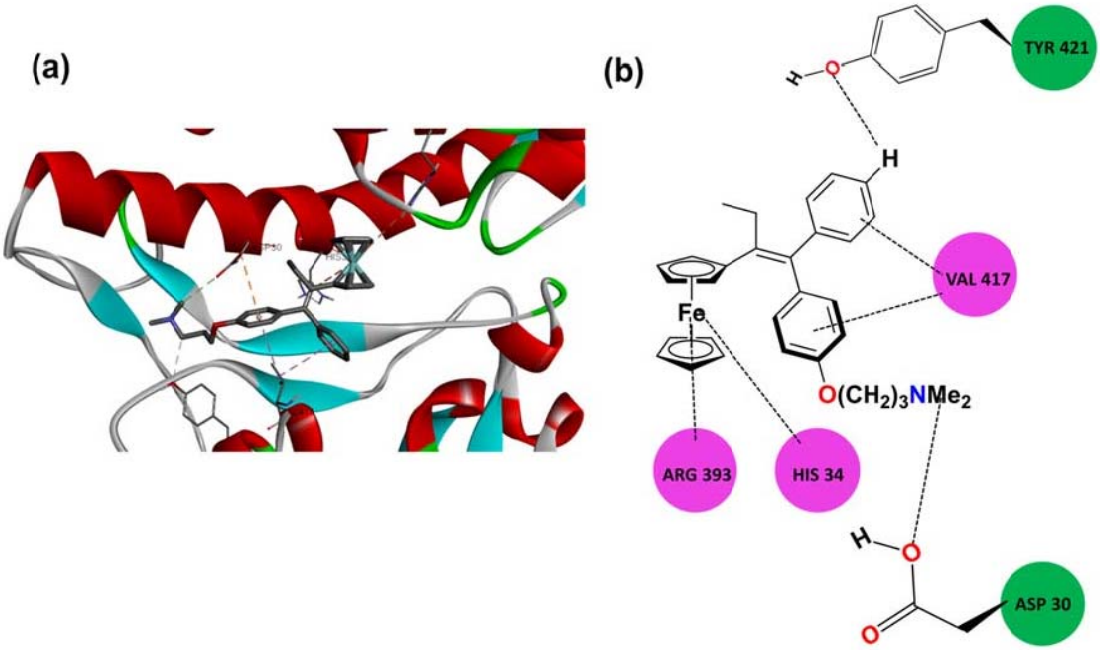

Fig. S3 - The best dock pose exhibiting non-covalent interactions between ferrocifen and the spike protein of SARS-CoV-2. (b) Schematic representation of showing the all the non-covalent interactions with TYR421, ASP30, VAL417, HIS34, ARG393 residues.

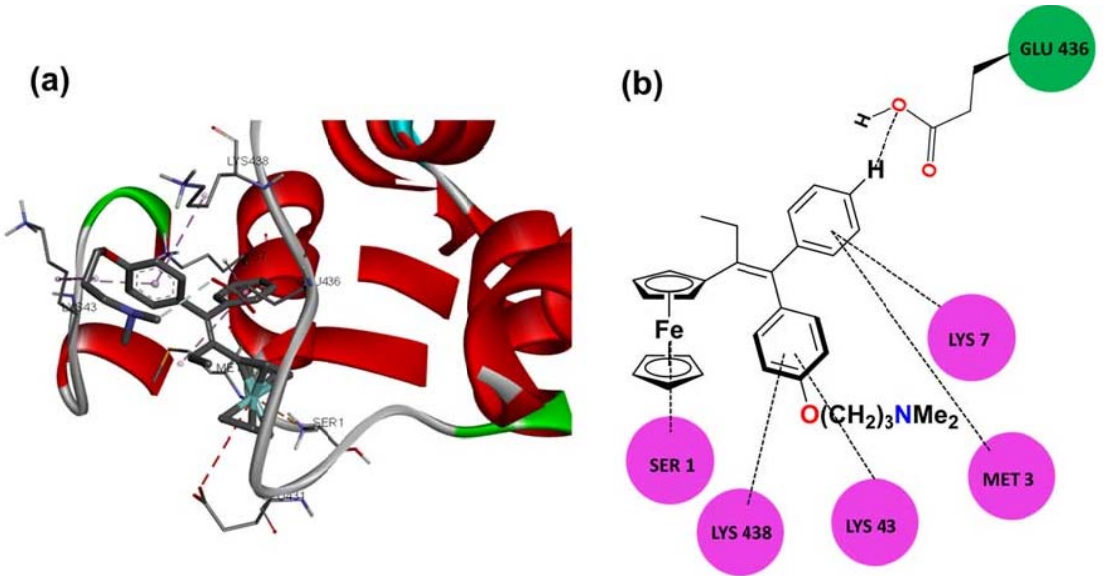

Fig. S4 - The best dock pose exhibiting non-covalent interactions between ferrocifen and the RdRp protein of SARS-CoV-2. (b) Schematic representation of showing the all the non-covalent interactions with GLU436, LYS7, MET3, LYS43, LYS438 and SER1 residues.

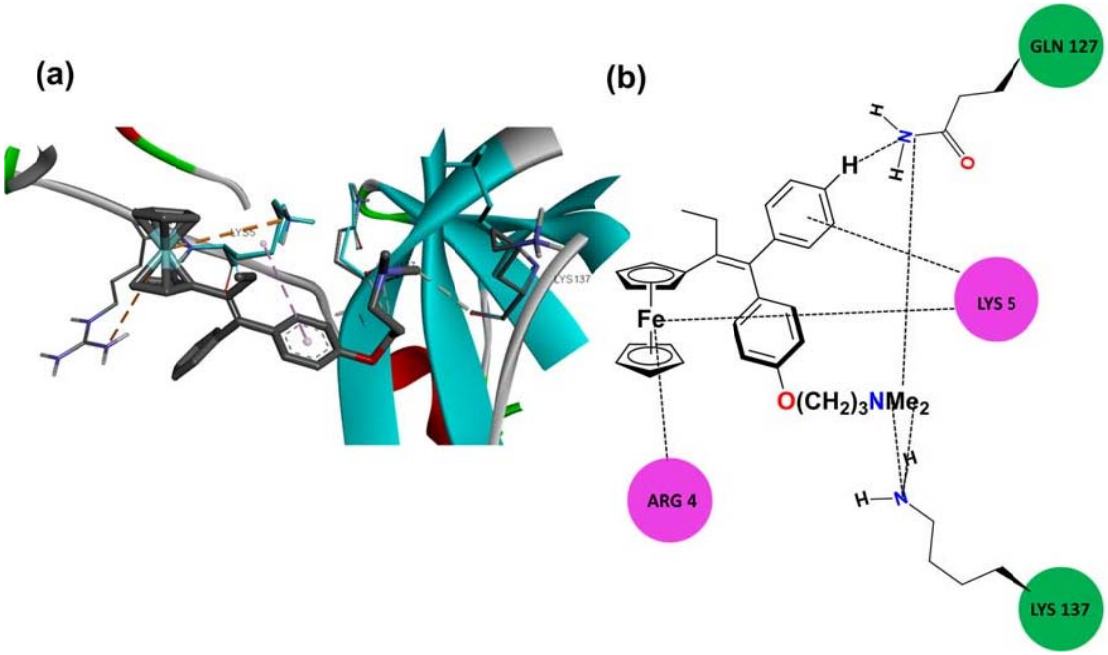

Fig. S5 - The best dock pose exhibiting non-covalent interactions between ferrocifen and the M_{pro} protein of SARS-CoV-2. (b) Schematic representation of showing the all the non-covalent interactions with GLN127, LYS137, LYS5 and ARG4 residues.

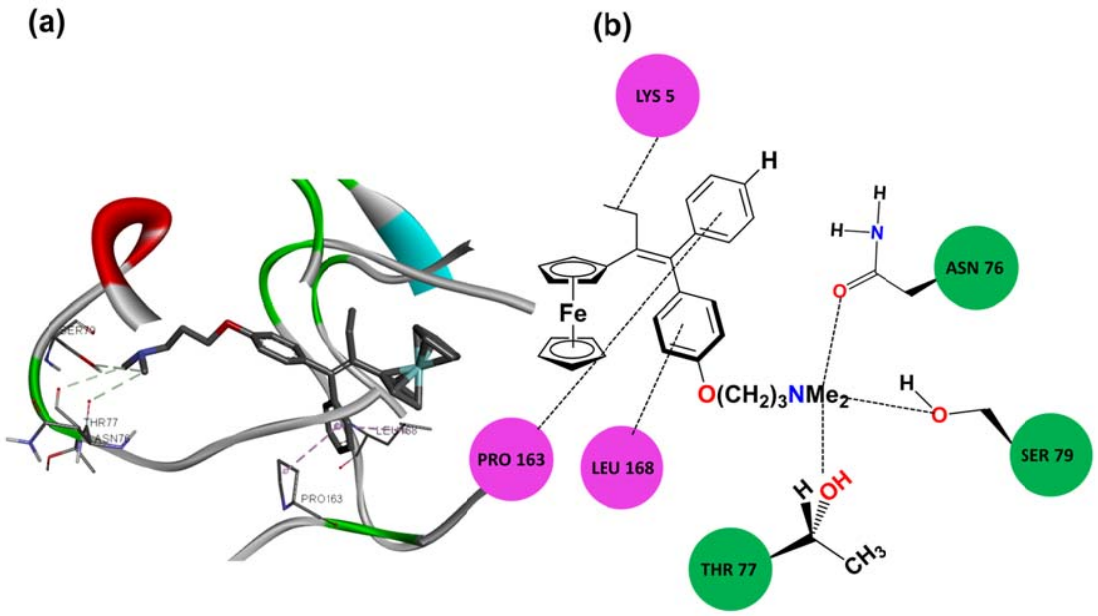

Fig. S6 - The best dock pose exhibiting non-covalent interactions between ferrocifen and the N protein of SARS-CoV-2. (b) Schematic representation of showing the all the non-covalent interactions with ASN76, SER79, THR77, PRO163, LEU168 and LYS5 residues.

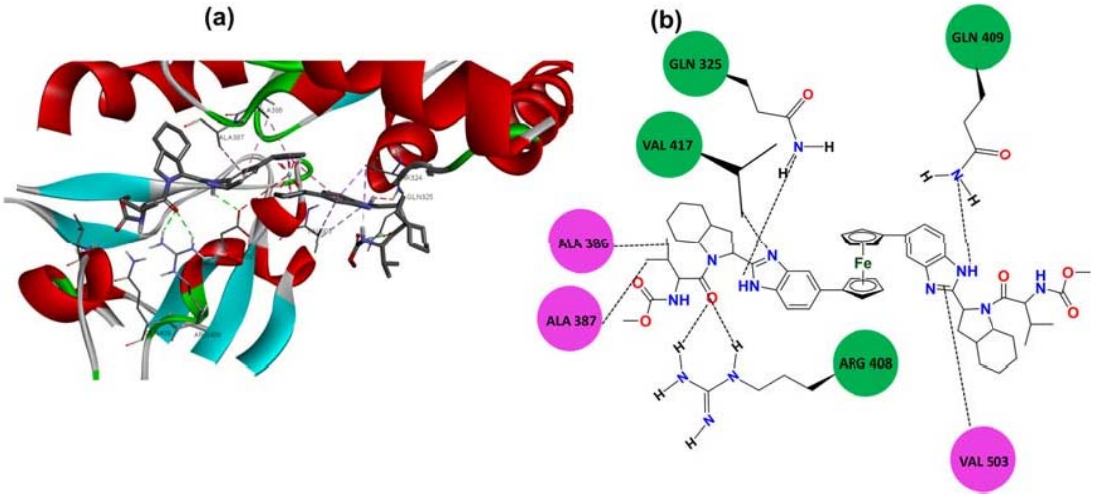

Fig. S7 - The best dock pose exhibiting non-covalent interactions between compound 1 and the spike protein of SARS-CoV-2. (b) Schematic representation of showing the all the non-covalent interactions with GLN325, VAL417, ARG408, GLN409, ALA386, ALA387 and VAL503 residues.

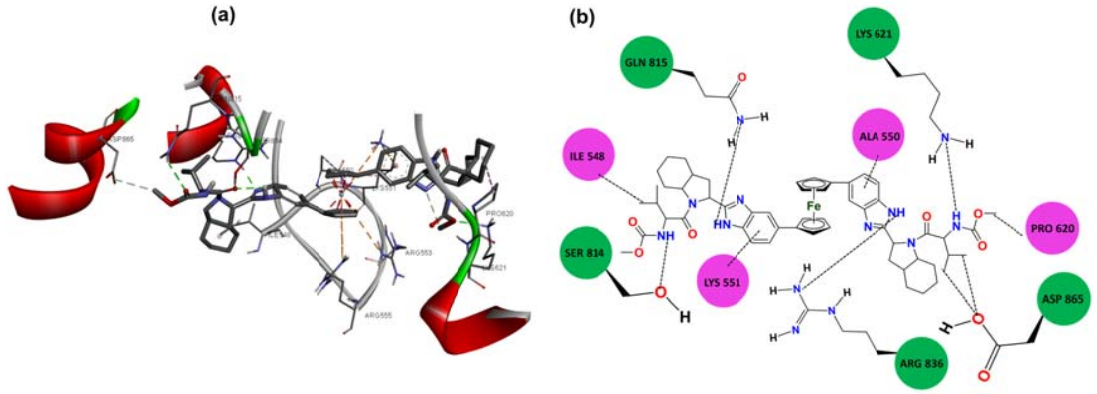

Fig. S8 - The best dock pose exhibiting non-covalent interactions between compound 1 and the RdRp protein of SARS-CoV-2. (b) Schematic representation of showing the all the non-covalent interactions with GLN815, SER814, ARG836, ASP865, LYS621, ILE548, LYS551, ALA550 and PRO620 residues.

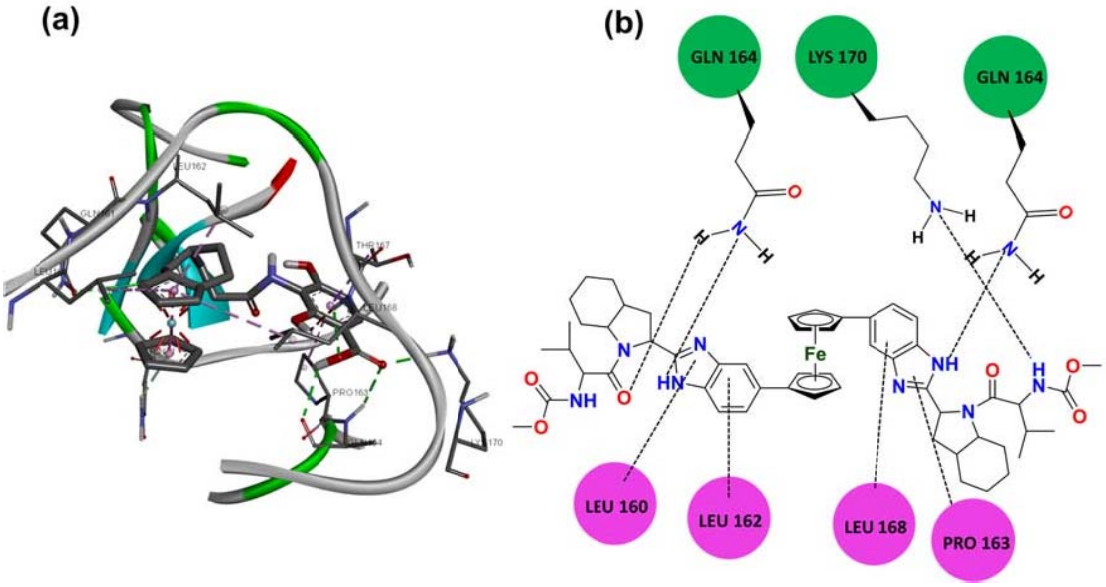

Fig. S9 - The best dock pose exhibiting non-covalent interactions between compound 1 and the N protein of SARS-CoV-2. (b) Schematic representation of showing the all the non-covalent interactions with GLN164, LYS170, GLN164, LEU160, LEU162, LEU168 and PRO163 residues.

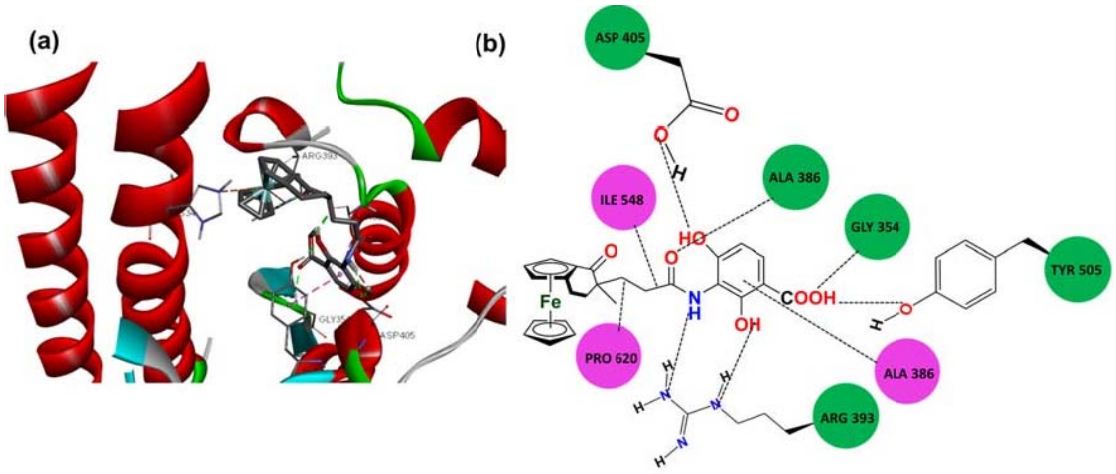

Fig. S10 - The best dock pose exhibiting non-covalent interactions between compound 2 and the spike protein of SARS-CoV-2. (b) Schematic representation of showing the all the non-covalent interactions with ASP405, ALA386, GLY354, ARG393, TYR505, ILE548, PRO620 and ALA386 residues.

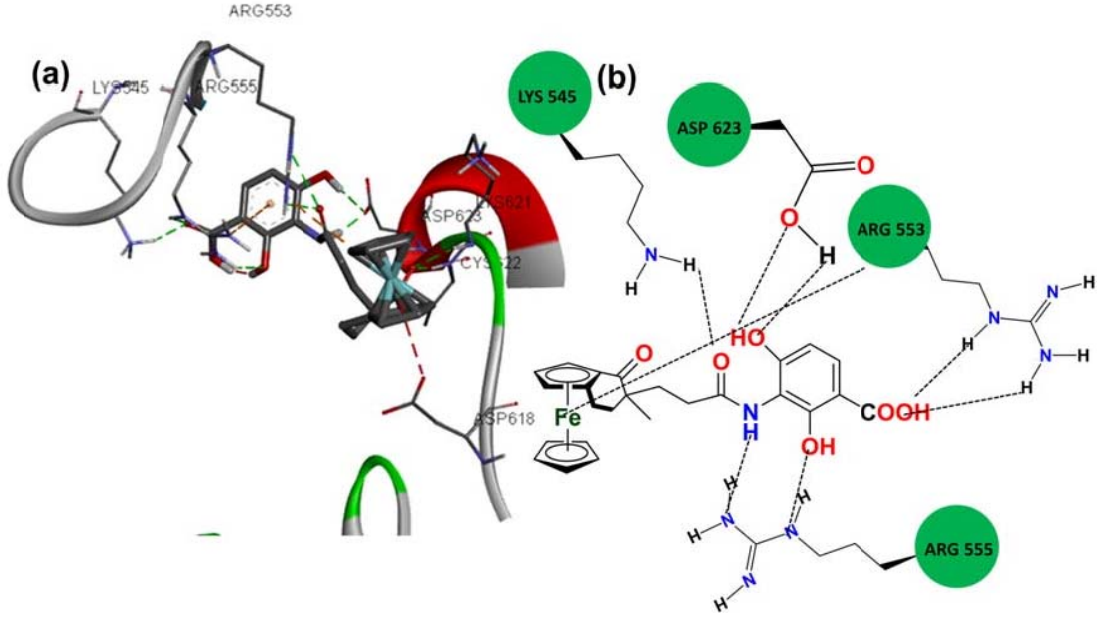

Fig. S11 - The best dock pose exhibiting non-covalent interactions between compound 2 and the RdRp protein of SARS-CoV-2. (b) Schematic representation of showing the all the non-covalent interactions with LYS545, ASP623, ARG553 and ARG555 residues.

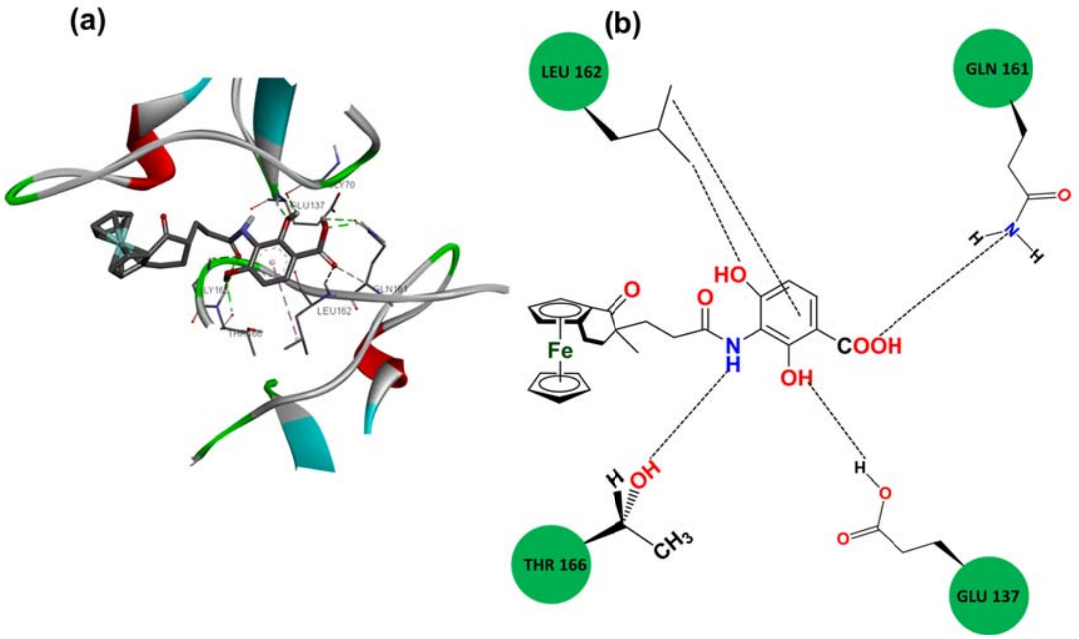

Fig. S12 - The best dock pose exhibiting non-covalent interactions between compound 2 and the N protein of SARS-CoV-2. (b) Schematic representation of showing the all the non-covalent interactions with LEU162, THR166, GLU137 and GLN161 residues.

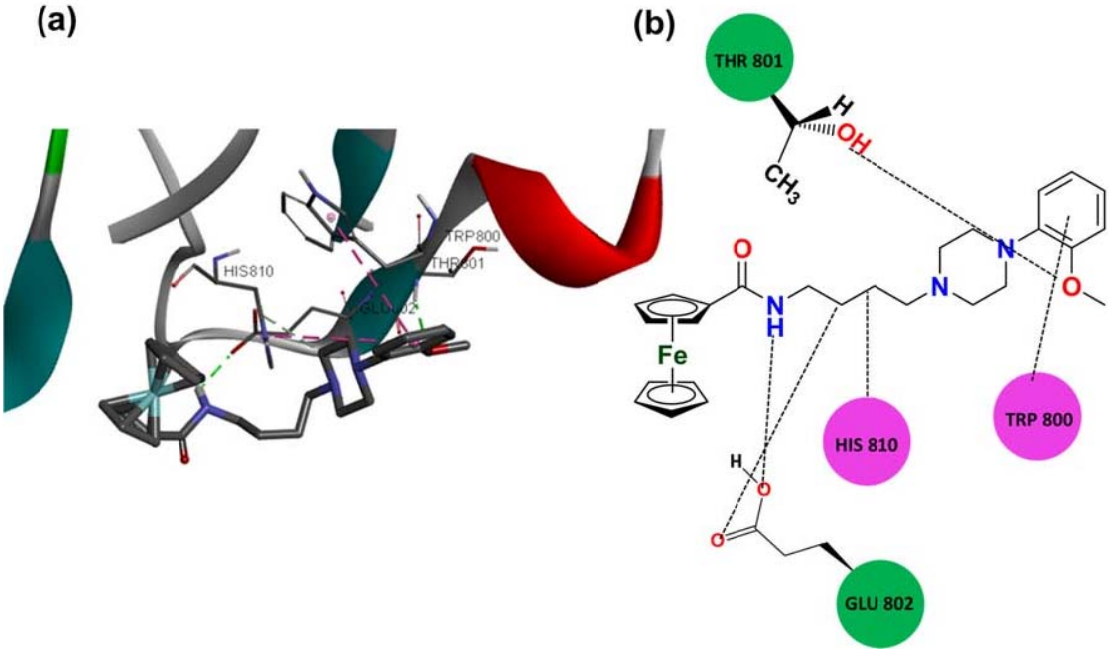

Fig. S13 - The best dock pose exhibiting non-covalent interactions between compound 3 and the RdRp protein of SARS-CoV-2. (b) Schematic representation of showing the all the non-covalent interactions with THR801, GLU802, HIS810 and TRP800 residues.

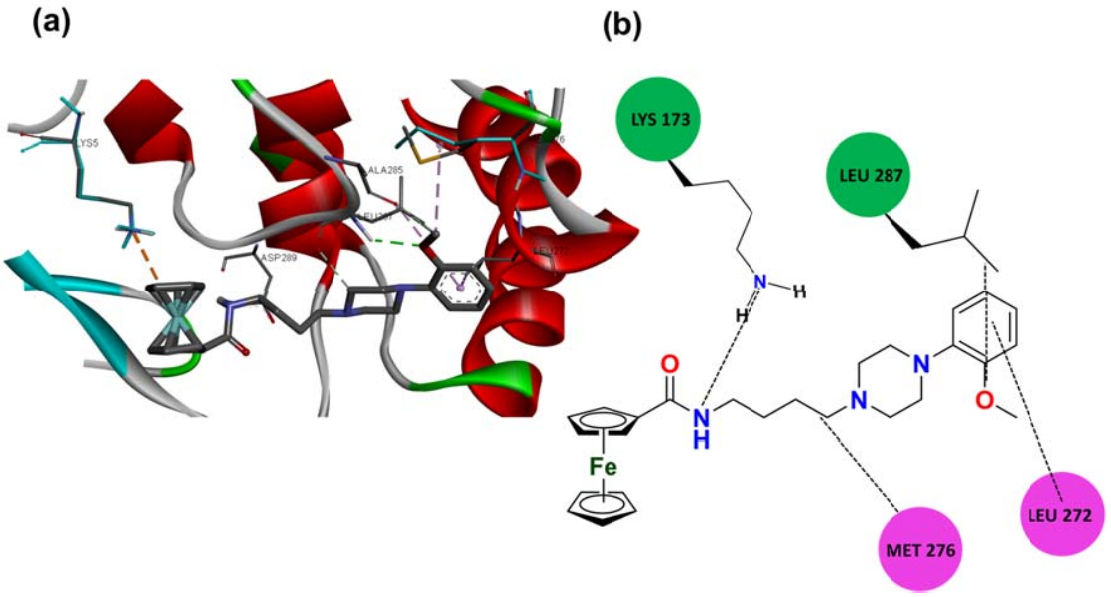

Fig. S14 - The best dock pose exhibiting non-covalent interactions between compound 3 and the M_{pro} protein of SARS-CoV-2. (b) Schematic representation of showing the all the non-covalent interactions with LYS173, LEU287, MET276 and LEU272 residues.

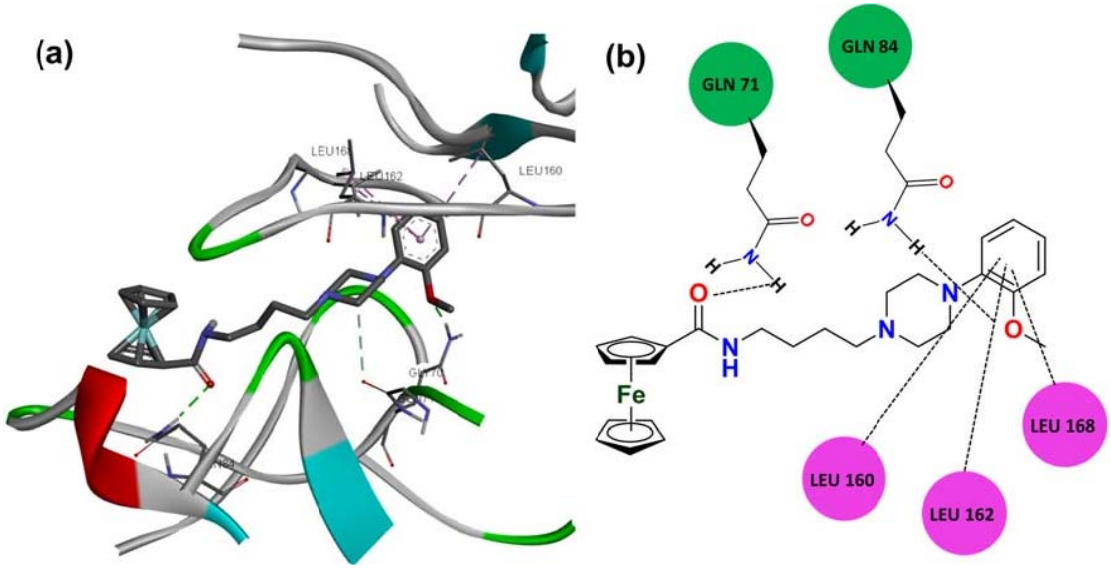

Fig. S15 - The best dock pose exhibiting non-covalent interactions between compound 3 and the N protein of SARS-CoV-2. (b) Schematic representation of showing the all the non-covalent interactions with GLN71, GLN84, LEU160, LEU162 and LEU168 residues.

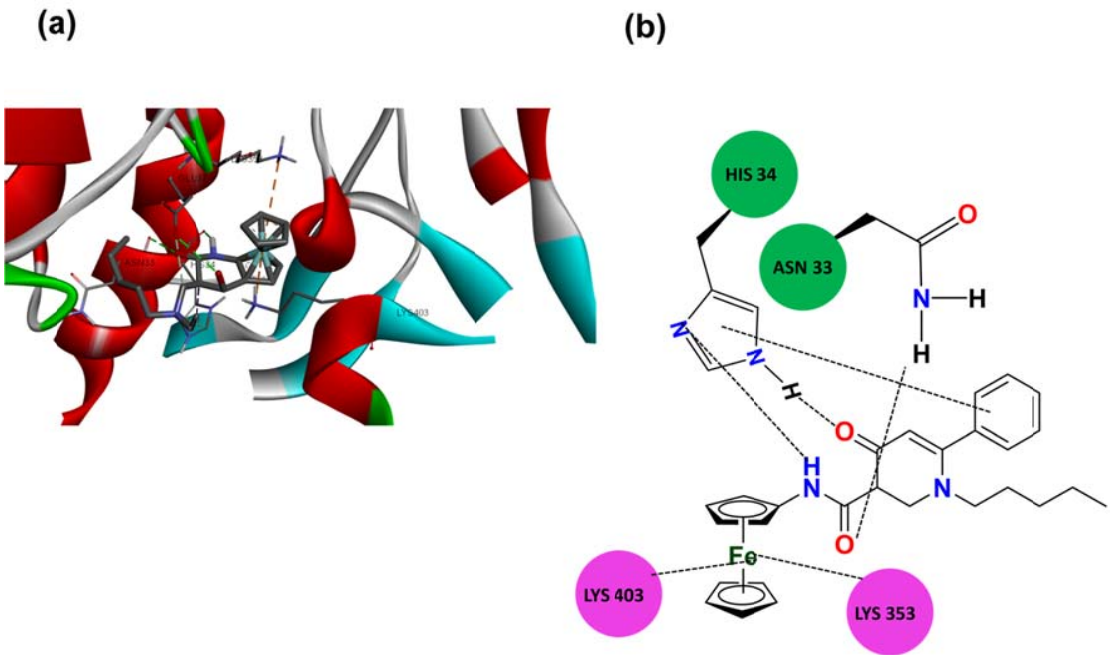

Fig. S16 - The best dock pose exhibiting non-covalent interactions between compound 4 and the spike protein of SARS-CoV-2. (b) Schematic representation of showing the all the non-covalent interactions with HIS34, ASN33, LYS403 and LYS353 residues.

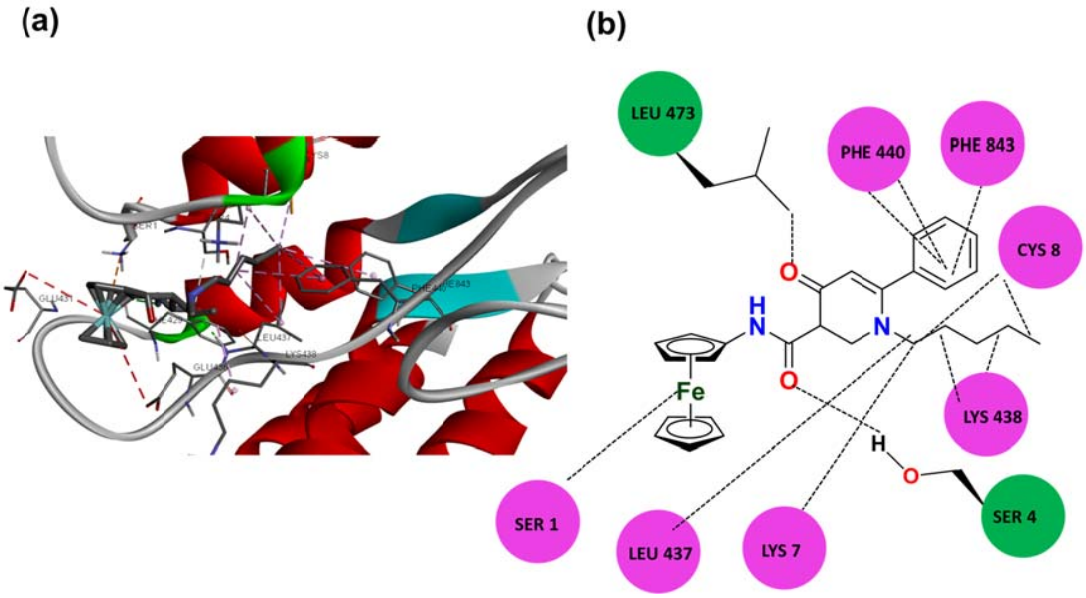

Fig. S17 - The best dock pose exhibiting non-covalent interactions between compound 4 and the RdRp protein of SARS-CoV-2. (b) Schematic representation of showing the all the non-covalent interactions with LEU473, SER4, PHE440, PHE843, CYS8, LYS438, LYS7, LEU437 and SER1 residues.

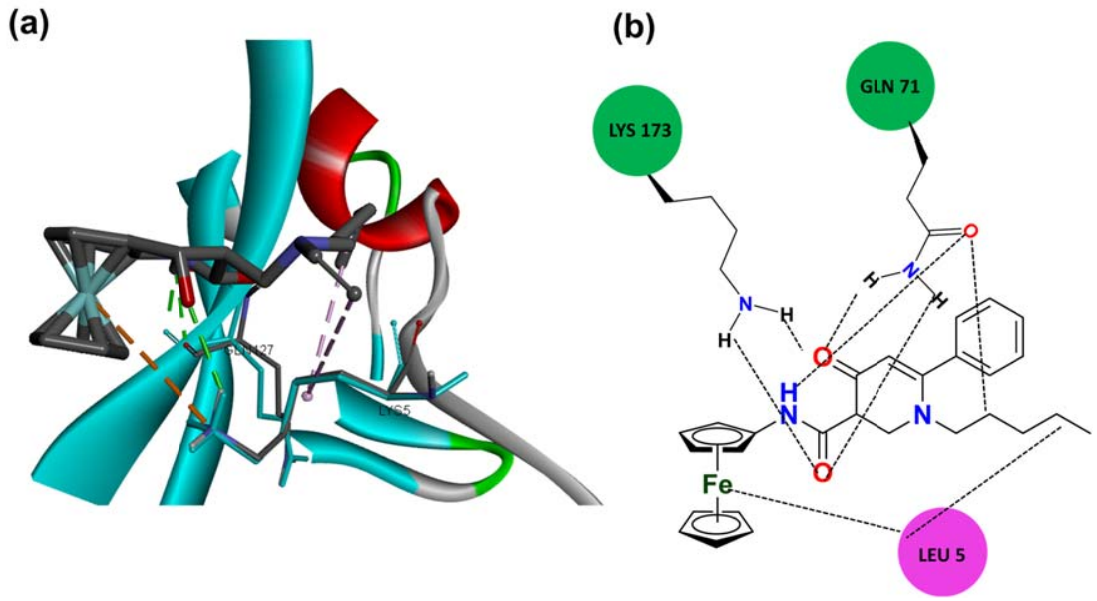

Fig. S18 - The best dock pose exhibiting non-covalent interactions between compound 4 and the M_{pro} protein of SARS-CoV-2. (b) Schematic representation of showing the all the non-covalent interactions with LYS173, GLN71 and LEU5 residues.

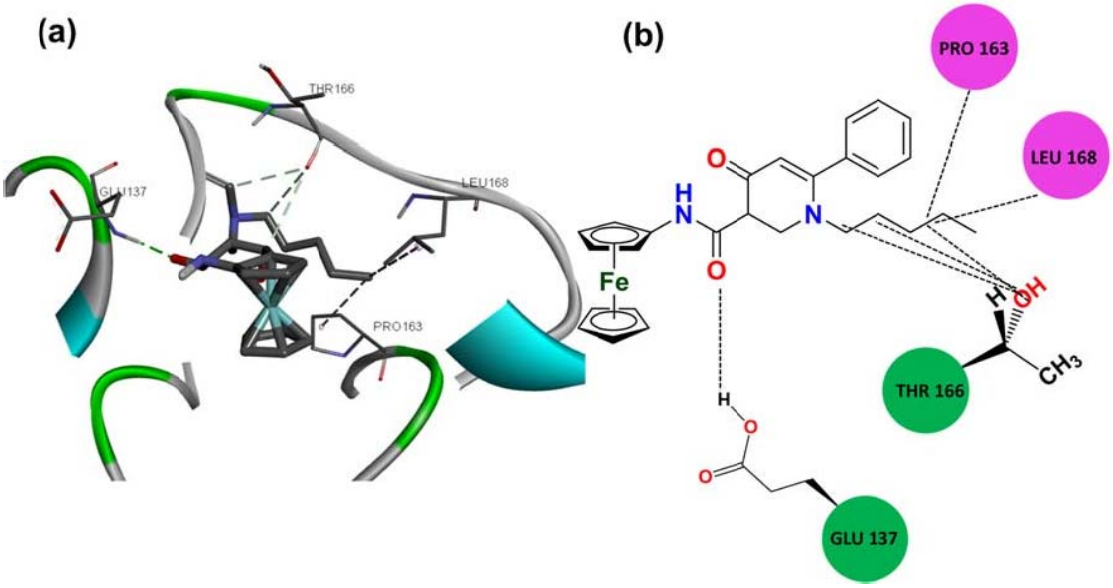

Fig. S19 - The best dock pose exhibiting non-covalent interactions between compound 4 and the N protein of SARS-CoV-2. (b) Schematic representation of showing the all the non-covalent interactions with GLU137, THR166, PRO163 and LEU168 residues.